Spin-entangled electrons in solid-state systems

2007 J. Phys.: Condens. Matter 19 233202

(http://iopscience.iop.org/0953-8984/19/23/233202)

IOP PUBLISHING JOURNAL OF PHYSICS: CONDENSED MATTER

J. Phys.: Condens. Matter **19** (2007) 233202 (24pp) doi:10.1088/0953-8984/19/23/233202

TOPICAL REVIEW

Spin-entangled electrons in solid-state systems

Guido Burkard[1]

Department of Physics and Astronomy, University of Basel, Klingelbergstrasse 82, CH-4056 Basel, Switzerland

Received 16 February 2007
Published 8 May 2007
Online at stacks.iop.org/JPhysCM/19/233202

Abstract

Entanglement is one of the fundamental resources for quantum information processing. This is an overview on theoretical work focused on the physics of the detection, production, and transport of entangled electron spins in solid-state structures.

(Some figures in this article are in colour only in the electronic version)

Contents

[1] Present address: Institute of Theoretical Physics C, RWTH Aachen, D-52056 Aachen, Germany.

0953-8984/07/233202+24$30.00

1. Introduction

1.1. Entanglement

Entanglement is among the fundamental resources for quantum information processing. A system composed of multiple parts $A, B, \ldots$ is entangled if it is in a pure[2] state ψ that cannot be described as a tensor product $\psi = \psi_A \otimes \psi_B \otimes \cdots$, where ψ_i denotes the wavefunction of part i. In what follows, we restrict our discussion to bipartite systems in which each of the two subsystems A and B is a single qubit for which we use spin $1/2$ notation (here, we are interested in electron spin based qubit realizations). In this case, there is, up to local operations, essentially only one maximally entangled state: the spin singlet

$$|S\rangle = \frac{1}{\sqrt{2}}\left(|\uparrow\downarrow\rangle - |\downarrow\uparrow\rangle\right), \tag{1}$$

where $|\sigma\sigma'\rangle = |\sigma\rangle \otimes |\sigma'\rangle$ and $\sigma, \sigma' = \uparrow, \downarrow$ represent the eigenstates of the spin operator along some fixed (say, z) direction. Note that outside the context of spin, the state equation (1) is also known as the *Bell state* $|\Psi_-\rangle \equiv |S\rangle$. The other three Bell states are (up to unimportant phases) related to $|\Psi_-\rangle$ by the unilateral application of one of the three Pauli matrices, $|\Psi_+\rangle = \sigma_z^{(1)}|\Psi_-\rangle$, $|\Phi_-\rangle = -\sigma_x^{(1)}|\Psi_-\rangle$, and $|\Phi_+\rangle = \sigma_z^{(1)}|\Phi_-\rangle = -\mathrm{i}\sigma_y|\Psi_-\rangle$.

The notion of entanglement goes back to Erwin Schrödinger, who called it the characteristic trait of quantum mechanics (Schrödinger 1935). Schrödinger's discourse was a reaction to the famous Einstein–Podolsky–Rosen (EPR) paper (Einstein *et al* 1935) in which the non-locality of an entangled state of two remote parts had been brought forward as evidence against the completeness of quantum mechanics. As was pointed out later by John Bell, the question whether nature allows a local realistic description can be expressed in terms of an inequality for a certain combination of correlation functions and can thus be decided experimentally if a source of entangled pairs (also called EPR pairs) like the one in equation (1) is available (Bell 1966, Mermin 1993). Such experiments have been carried out using the two linear polarizations of photons as the 'qubit states' (Aspect *et al* 1982), providing strong evidence against local realism and for the completeness of quantum mechanics as a description of nature.

The non-locality of a system in state equation (1) can be viewed as a limitation since it prohibits any local description. However, from a quantum information point of view, entanglement and non-locality are 'features' rather than 'bugs' of quantum mechanics. This is so because entanglement between remote parties (A and B) in a quantum communications setting can be used as a resource for a variety of quantum protocols (Bennett and DiVincenzo 2000). Among these are quantum teleportation, i.e., the faithful transmission of a quantum state using a classical channel plus previously shared entanglement (Bennett *et al* 1993), some variants of quantum key distribution (Ekert 1991), i.e., the generation of an unconditionally secure cryptographic key using EPR pairs, and quantum dense coding (Bennett and Wiesner 1992), i.e., the transmission of two classical bits by sending only one qubit and using one EPR pair. This list is by no means exhaustive: given that quantum channels can also be noisy, there exists an entire family of quantum protocols (Devetak *et al* 2004). In addition to the aforementioned experimental test of Bell's inequalities (Aspect *et al* 1982), several quantum communication protocols have been realized experimentally with entangled photons, among them dense coding (Mattle *et al* 1996), quantum teleportation (Bouwmeester *et al* 1997, Boschi *et al* 1998), and quantum cryptography (Gisin *et al* 2002).

[2] The definition of mixed state entanglement is somewhat more general and will be discussed further below.

1.2. Electron spin entanglement

The electron spin is a natural two-level system, which makes it an ideal candidate for a solid-state qubit (Loss and DiVincenzo 1998). Two electron spin qubits, each localized in one of two adjacent semiconductor quantum dots, can be coupled via the Heisenberg exchange interaction due to virtual electron tunnelling between the quantum dots (Burkard *et al* 1999). Experimentally, there has been remarkable progress towards electron spin qubits in structures such as quantum dots: the storage, preparation, coherent manipulation of a single electron spin in a quantum dot and the controlled coupling of two spins located in separate dots has been demonstrated experimentally (Hanson *et al* 2006). This article is a review of work dedicated to the question whether EPR pairs consisting of two electrons with entangled spins could be used perform those quantum protocols and to test Bell's inequalities and in a solid-state system. Since the use of entangled electron spin pairs in solid-state structures was theoretically proposed and analysed (Burkard *et al* 2000), there has been a growing activity aimed at understanding physical mechanisms that generate spin-entangled electrons in mesoscopic conductors. On the experimental side, electron spin entanglement, the violation of Bell's inequalities, or the realization of a quantum communication protocol with electron spins in a solid have not been reported so far, but experiments are still underway in this direction. One may also envision the conversion of spin entanglement of localized (Gywat *et al* 2002) or mobile (Cerletti *et al* 2005) electrons an efficient and deterministic means to generate polarization-entangled photons.

Entanglement is not uncommon in solid-state systems. On the contrary, entanglement is the rule rather than the exception in the low-energy states (say, the ground state) of interacting many-particle systems. However, such 'generic' entangled states are not necessarily useful for quantum information processing. A criterion for the usefulness as a resource is that there must be a realizable physical mechanism to extract and separate a 'standard' pair of entangled particles such as the EPR pair in equation (1) from the many-body system in such a way that the two particles can be used for quantum communication. This is often complicated by the indistinguishability of the particles: in this case, a state that 'looks entangled' when written out in first quantized notation might not be entangled in an operational sense (i.e., there may not be any physical procedure that separates the particle while maintaining their entanglement). Mathematically, this is related to the fact that the Hilbert space for several identical particles is not a tensor product when proper antisymmetrization is taken into account. Measures of entanglement which take into account the indistinguishability of particles have been introduced (Dowling *et al* 2006, Schliemann *et al* 2001a, 2001b, Wiseman and Vaccaro 2003).

1.3. What is not covered by this review

This article is about spin entanglement between two electrons in solid-state structures. It does not cover orbital entanglement of charge carriers, such as electron–hole entanglement (see Beenakker 2006), (orbital) exciton entanglement (Hohenester 2002), orbital entanglement between electrons (Samuelsson *et al* 2003), and entanglement between encoded spin states (Taylor *et al* 2005). Another review on some of the topics covered here is Egues *et al* (2003).

2. Detection of spin entanglement

What physically measurable consequences does the entanglement of two electron spins in an entangled state like equation (1) have? How can one distinguish an entangled pair of electron

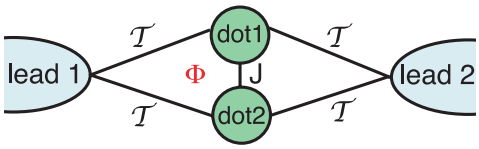

Figure 1. Setup for detecting entanglement of two localized electrons in two tunnel-coupled quantum dots (Loss and Sukhorukov 2000). Each dot is filled with one electron and is coupled via a tunnelling amplitude $\mathcal{T}$ to each of the two leads. In addition, the two quantum dots are tunnel-coupled amongst each other, which leads to an inter-dot exchange coupling J, energetically favouring the entangled singlet state to the triplet states of the two spins. For the detection of this entanglement, the current and/or current fluctuations from lead 1 to lead 2 need to be observed as a function of the magnetic flux Φ threading the loop enclosed by the tunnelling paths.

spins (or a stream thereof) from an unentangled one? We will describe several tests for spin entanglement in this section. One of the most straightforward methods would be to test Bell's inequality directly (in fact, such proposals have been made for electron spins in solids, as we will briefly report in section 2.8, below). However, testing Bell's inequality involves measuring single electron spins one by one along at least three non-collinear quantization axes, which is by no means a simple practical task.

There is an alternative to direct Bell tests which allows one to gain information about spin entanglement from a charge measurement by exploiting the Fermi statistics of the electrons, giving rise to a unique relation between the symmetry of the orbital state and the two-electron spin state. Such charge measurements can be of two different types: electrostatic (via a nearby quantum point contact or single-electron transistor) or transport (measurements of the current and/or its fluctuations).

2.1. Localized electrons: coupled quantum dots

We first consider a setup that can be used to probe the entanglement of two electrons localized in a double dot (as shown in figure 1) by measuring a transport current and its fluctuations, or current noise (Loss and Sukhorukov 2000). The parameter regime of interest is that of weak coupling between the double dot and the incoming and outgoing leads (which are held at the chemical potentials $\mu_{1,2}$) with tunnelling amplitude $\mathcal{T}$, where the dots are shunted in parallel. Moreover, the parameters need to lie in (i) the Coulomb blockade regime (Kouwenhoven *et al* 1997) where the charge on the dots is quantized and (ii) the cotunnelling regime (Averin and Nazarov 1992), where single-electron tunnelling is suppressed by energy conservation. The cotunnelling regime is defined by $U > |\mu_1 \pm \mu_2| > J > k_B T, 2\pi\nu\mathcal{T}^2$, with U the charging energy on a single dot, ν the density of states in the leads, and J the exchange coupling between the spins on the two dots. The electric current in the cotunnelling regime is generated by a coherent virtual process where one electron tunnels from one of the dots to one of the leads (say, lead 2) and then a second electron tunnels from the other lead (in our example, lead 1) to the same dot. For bias voltages exceeding the exchange coupling, $|\mu_1 - \mu_2| > J$, both elastic and inelastic cotunnelling are permitted. It is assumed that $\mathcal{T}$ is sufficiently small for the double-dot system to equilibrate after each tunnelling event. An electron can either pass through the upper or through the lower dot, such that a closed loop is formed by these two paths. An externally applied magnetic field B then induces a magnetic flux $\Phi = AB$ that threads this loop (with area A) and leads to an Aharonov–Bohm (AB) phase $\phi = e\Phi/\hbar$ between the upper and the lower path. The AB phase influences the quantum interference between the two paths. Such a transport setting is sensitive to the spin symmetry of the two-electron state on the double dot;

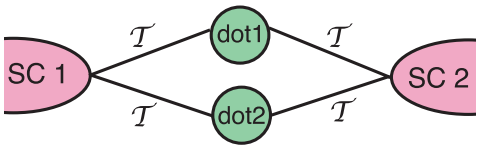

Figure 2. The setup described in Choi *et al* (2000). Two quantum dots are connected in a parallel shunt between two SC contacts (tunnelling amplitude $\mathcal{T}$), without any direct tunnel coupling between the quantum dots.

if the two electrons on the double-dot are in the singlet state $|S\rangle$, as in equation (1), then the tunnelling current acquires an additional phase of π leading to a sign reversal of the coherent contribution compared to that for triplets,

$$|T_{-1}\rangle = |\downarrow\downarrow\rangle = \frac{1}{\sqrt{2}}\left(|\Phi_+\rangle - |\Phi_-\rangle\right), \tag{2}$$

$$|T_0\rangle = \frac{1}{\sqrt{2}}\left(|\uparrow\downarrow\rangle + |\downarrow\uparrow\rangle\right) = |\Psi_+\rangle, \tag{3}$$

$$|T_{+1}\rangle = |\uparrow\uparrow\rangle = \frac{1}{\sqrt{2}}\left(|\Phi_+\rangle + |\Phi_-\rangle\right). \tag{4}$$

This phase is reflected in the sign of an interference term in the average current in the cotunnelling regime (Loss and Sukhorukov 2000)

$$I = e\pi\nu^2\mathcal{T}^4\,\frac{\mu_1 - \mu_2}{\mu_1\mu_2}\,(2 \pm \cos\phi), \tag{5}$$

where the upper (lower) sign belongs to the triplet (singlet) states in the double dot. The fluctuations of the electric current (shot noise) follow Poissonian statistics with noise power $S(0) = -e|I|$, and thus they inherit the dependence on the spin state from that of the average current. Note that the singlet is maximally entangled (see above) while one of the triplets ($|T_0\rangle$) is entangled (hence, $|T_0\rangle$ is also an EPR pair) and the other two ($|T_\pm\rangle$) are not entangled. Therefore, if the singlet can be distinguished from the triplet, then at least for one outcome (singlet), entanglement has been detected unambiguously.

For finite frequencies the shot noise is proportional to the same statistical factor (Loss and DiVincenzo 1998), $S(\omega) \propto (2 \pm \cos\phi)$, where the odd part of $S(\omega)$ leads to slowly decaying oscillations of the noise in real time, $S(t) \propto \sin(\mu t)/\mu t$, $\mu = (\mu_1 + \mu_2)/2$. This decay is due to a charge imbalance between the two dots during a time $\Delta t \approx \mu^{-1}$. A general study of the quantum shot noise in cotunnelling through coupled quantum dot systems can be found in Sukhorukov *et al* (2001).

2.2. *Coupled dots with superconducting contacts*

A setup similar to the one shown in figure 1 with two quantum dots, but connected to superconducting (SC) leads (with tunnelling amplitude $\mathcal{T}$), and without direct tunnel coupling between the dots, has been considered in Choi *et al* (2000). This setup is shown in figure 2. Two main results have been reported for this system: the coupling to the SC leads (i) energetically favours an entangled singlet state on the dots, and (ii) provides a mechanism for detecting the spin state via the Josephson current through the double dot system.

The lowest-order tunnelling effects $\propto \mathcal{T}^4$ are captured with the following Heisenberg spin Hamiltonian (Choi *et al* 2000),

$$H_{\rm eff} \approx J(1 + \cos\varphi)\,\left(\mathbf{S}_1 \cdot \mathbf{S}_2 - \tfrac{1}{4}\right), \tag{6}$$

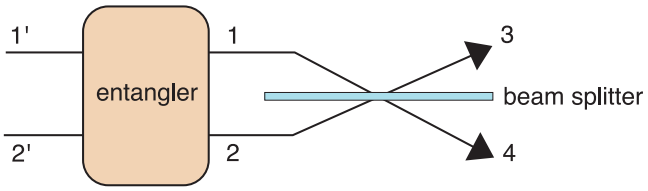

Figure 3. The beam-splitter setup. An entangler (see section 3) transforms uncorrelated electrons (here schematically indicated as leads $1'$ and $2'$) into pairs of electrons in the entangled singlet (triplet) state $|\Psi_{\mp}\rangle$, which are injected into leads 1, 2 (one electron per lead). The entanglement of the spin singlet can then be detected in an interference measurement with the beam splitter. Since the orbital wave function of the singlet is symmetric, the electrons leave the scattering region preferably in the same lead (3 or 4), cf table 1. This correlation of the particle number ('bunching') manifests itself in an enhancement of the shot noise by a factor of 2 in the outgoing leads.

with an exchange coupling $J \approx 2\mathcal{T}^2/\epsilon$, where ϵ is the energy separation between the quantum dot state and the Fermi level, and φ is the average phase difference between the two SC reservoirs. The exchange coupling J can be controlled by tuning the external parameters $\mathcal{T}$ and φ, thus providing an implementation of an entangler (see section 3 below). The two-spin state (singlet or triplet) on the double dot can be probed with a transport measurement by forming a SQUID with the device shown in figure 2 combined in a parallel shunt with one additional (ordinary) Josephson junction with coupling J' and phase difference θ. The SC current I_S in such a ring circuit is then found to be (Choi *et al* 2000)

$$I_S/I_J = \begin{cases} \sin(\theta - 2\pi\phi/\phi_0) + (J'/J)\sin\theta, & \text{singlet,} \\ (J'/J)\sin\theta, & \text{triplets,} \end{cases} \tag{7}$$

where $I_J = 2eJ/\hbar$, ϕ is the magnetic flux threading the SQUID loop, and ϕ_0 the SC flux quantum. By ramping a dc current I through the ring until the SC switches to its normal state at $|I| > I_c$ and a finite voltage V appears, the spin- and flux-dependent critical current $I_c = \max_\theta\{|I_S|\}$ can be determined.

2.3. Mobile electrons: beam splitter shot noise

In the preceding section 2.1, we have discussed the detection of entanglement in the ground state of two electrons *localized* in a double-dot structure via the electric current and noise across the structure. Now, we turn to the detection of spin entanglement of *mobile* electron spins. For this purpose, the electron pair to be tested will itself carry the electric current. It turns out that pairwise spin entanglement between electrons in two mesoscopic conductors can be detected in the fluctuations of the charge current after transmission through an electronic beam splitter (Burkard *et al* 2000) as shown schematically in figure 3. As we discuss in detail below, the singlet EPR pair equation (1) produces an enhancement of the shot noise power ('bunching' behaviour), whereas the triplets $|T_{0,\pm1}\rangle$, equations (2)–(4) lead to a suppression of noise ('antibunching').

This result can be understood by inspection of table 1. For indistinguishable, fermionic particles such as electrons, the antisymmetry of the total wavefunction (spin and orbit combined) dictates that the orbital wavefunction must be symmetric if the spin wavefunction is antisymmetric (as in the case of the spin singlet) and vice versa for the triplets. Assuming that each conductor has only one channel (which we simply denote $|n\rangle$, where n is the label of the contact), we can easily enumerate all possible final states with the prescribed symmetry. The task of the beam splitter is to distribute the particles over these possible states in order to

Table 1. Number statistics for fermions at a symmetric beam splitter.

State	Spin wavefunction	Orbital wavefunction	Final states (orbit)	$\langle \delta N_3^2 \rangle$	Entanglement
$\|S\rangle$	Antisymmetric	Symmetric	$\|33\rangle$, $\|44\rangle$	1	Yes
$\|T_0\rangle$	Symmetric	Antisymmetric	$\|34\rangle - \|43\rangle$	0	Yes
$\|T_\pm\rangle$	Symmetric	Antisymmetric	$\|34\rangle - \|43\rangle$	0	No
Distinguishable	—	—	$\|33\rangle$, $\|44\rangle$, $\|34\rangle$, $\|43\rangle$	1/2	Possible

probe the symmetry properties of the wavefunction. For a symmetric beam splitter where the transmission and reflection probabilities are both $1/2$ (for the general case, see below), each of these states allowed by symmetry is filled with equal probability. Then, it is easy to obtain the mean and variance of the probability distribution for $N = N_3$, the number of outgoing electrons in lead $n = 3$ (Loudon 1998). The mean is always $\langle N \rangle = 1$ and does not contain any information on the statistics or entanglement of the ingoing state. We therefore do not expect that here (unlike for the localized electrons in section 2.1) the average electric current will contain any information about the spin state. However, the variance $\langle \delta N_3^2 \rangle$ vanishes for triplets because there is only one possible final state and thus fluctuations are impossible (this behaviour is called 'antibunching' of particles), while for the singlet $\langle \delta N_3^2 \rangle = 1$, which is twice as large as expected for (classical) distinguishable particles (also known as 'bunching'). Note that for bosons (e.g., photons), since the total wavefunction must be symmetric, the role of singlet and triplet are interchanged. In fact, for bosons, this effect is well known as the Hong–Ou–Mandel dip in interferometry with entangled photon pairs (Hong *et al* 1987). Bunching behaviour for (unentangled) bosons also underlies the famous Hanbury–Brown and Twiss experiment (Hanbury Brown and Twiss 1956).

Here, we are interested in the fact that particle bunching, i.e., the enhancement of the fluctuations of the electron current, is only possible for an entangled state (the singlet) and thus particle bunching is a unique signature for entanglement. Nothing of this sort can be said for antibunching, since there are both entangled and unentangled triplets. This result can be extended to non-maximally entangled states (see below for a quantitative discussion); we only anticipate here that in table 1 we find $\langle \delta N_3^2 \rangle \leqslant 1/2$ for all unentangled states. Conversely, a number fluctuation $\langle \delta N_3^2 \rangle > 1/2$ can be interpreted as a signature of entanglement. However, we still need to relate $\langle \delta N_3^2 \rangle$ to a physically measurable quantity (the shot noise power at low frequencies).

Let us now turn to the physical setup (figure 3) with a beam splitter where electrons have an amplitude t to be interchanged (without mutual interaction) such that $0 < |t|^2 < 1$. Shot noise of the electric current in such beam splitter devices has been studied for normal (unentangled) electrons both in theory (Büttiker 1990, 1992, Martin and Landauer 1992, Torrès and Martin 1999) and experiment (Henny *et al* 1999, Liu *et al* 1998, Oliver *et al* 1999). Recent experiments have investigated the sign of the cross-correlations after transmission of fermions through a beam splitter and the distinction between the effects from Fermi statistics and other effects such as noisy injection and interactions (Chen and Webb 2006, Oberholzer *et al* 2006). These experiments have been performed in semiconductor nanostructures with geometries that are very similar to the setup proposed in figure 3, but without any entangler device.

The effect of interactions in the leads will be addressed in section 4 below. To calculate the shot noise of spin-entangled electrons, standard scattering theory (Blanter and Büttiker 2000, Büttiker 1990, 1992) was extended to a situation with entanglement (Burkard *et al* 2000). The entangled two-electron state injected into two distinct leads 1 and 2 can be written in second

quantized notation as

$$|\Psi_\pm\rangle \equiv |\psi^{\mathrm{t/s}}_{\mathbf{n}\mathbf{n}'}\rangle = \frac{1}{\sqrt{2}}\left(a^\dagger_{\mathbf{n}\uparrow}a^\dagger_{\mathbf{n}'\downarrow} \pm a^\dagger_{\mathbf{n}\downarrow}a^\dagger_{\mathbf{n}'\uparrow}\right)|\psi_0\rangle, \tag{8}$$

where s and t stand for the singlet and triplet, $|\psi_0\rangle$ for the filled Fermi sea, and $\mathbf{n} = (\mathbf{q}, l)$, where $\mathbf{q}$ denotes the momentum and l the lead quantum number of an electron. The operator $a^\dagger_{\mathbf{n}\sigma}$ creates an electron in state $\mathbf{n}$ with spin σ. Alternatively, we can use the quantum numbers $\mathbf{n} = (\varepsilon_n, n)$, with the electron energy ε_n instead of the momentum as the orbital quantum number in equation (8). The operator $a^\dagger_{\alpha\sigma}(\varepsilon)$ then creates an incoming electron in lead α with spin σ and energy ε. After being injected, the two electrons are no longer distinguishable from the electrons that had been in the leads before, and consequently the two electrons retrieved from the system will, in general, not be 'the same' as the ones injected. When extending the theory for the current correlations in a multiterminal conductor (Büttiker 1990, 1992) to the case of entangled scattering states, we need to take into account that Wick's theorem cannot be applied any more. The current operator for lead α of a multiterminal conductor is

$$I_\alpha(t) = \frac{e}{h\nu}\sum_{\varepsilon\varepsilon'\sigma}\left[a^\dagger_{\alpha\sigma}(\varepsilon)a_{\alpha\sigma}(\varepsilon') - b^\dagger_{\alpha\sigma}(\varepsilon)b_{\alpha\sigma}(\varepsilon')\right]\exp\left[\mathrm{i}(\varepsilon-\varepsilon')t/\hbar\right], \tag{9}$$

with the operators $b_{\alpha\sigma}(\varepsilon)$ for the outgoing electrons, that are related to the operators $a_{\alpha\sigma}(\varepsilon)$ for the incident electrons via $b_{\alpha\sigma}(\varepsilon) = \sum_\beta s_{\alpha\beta}a_{\beta\sigma}(\varepsilon)$, where $s_{\alpha\beta}$ is the scattering matrix. Here, the scattering matrix is assumed to be spin and energy independent. For a discrete energy spectrum in the leads, the operators $a_{\alpha\sigma}(\varepsilon)$ can be normalized such that $\{a_{\alpha\sigma}(\varepsilon), a^\dagger_{\beta\sigma'}(\varepsilon')\} = \delta_{\sigma\sigma'}\delta_{\alpha\beta}\delta_{\varepsilon\varepsilon'}/\nu$, where the Kronecker symbol $\delta_{\varepsilon\varepsilon'}$ equals 1 if $\varepsilon = \varepsilon'$ and 0 otherwise, and where ν denotes the density of states in the leads. As mentioned before, we assume for the moment that each lead consists of only a single quantum channel; a more general treatment will be discussed in section 2.4 below. The current operator equation (9) can now be written in terms of the scattering matrix as

$$I_\alpha(t) = \frac{e}{h\nu}\sum_{\varepsilon\varepsilon'\sigma}\sum_{\beta\gamma}a^\dagger_{\beta\sigma}(\varepsilon)A^\alpha_{\beta\gamma}a_{\gamma\sigma}(\varepsilon')\mathrm{e}^{\mathrm{i}(\varepsilon-\varepsilon')t/\hbar}, \tag{10}$$

$$A^\alpha_{\beta\gamma} = \delta_{\alpha\beta}\delta_{\alpha\gamma} - s^*_{\alpha\beta}s_{\alpha\gamma}. \tag{11}$$

The current–current correlator between $I_\alpha(t)$ and $I_\beta(t)$ in two leads $\alpha, \beta = 1, \ldots, 4$ of the beam splitter is then

$$S^\chi_{\alpha\beta}(\omega) = \lim_{\tau\to\infty}\frac{h\nu}{\tau}\int_0^\tau \mathrm{d}t\,\mathrm{e}^{\mathrm{i}\omega t}\,\mathrm{Re}\,\mathrm{Tr}\left[\delta I_\alpha(t)\delta I_\beta(0)\chi\right], \tag{12}$$

where $\delta I_\alpha = I_\alpha - \langle I_\alpha\rangle$, $\langle I_\alpha\rangle = \mathrm{Tr}(I_\alpha\chi)$ and χ is the density matrix of the injected electron pair. Here, we are interested in the zero-frequency correlator $S_{\alpha\beta} \equiv S^\chi_{\alpha\beta}(0)$. In order not to overburden our notation, we omit the dependence on χ in what follows. If we substitute $\chi = |\Psi_\pm\rangle\langle\Psi_\pm|$ we obtain

$$S_{\alpha\beta} = \frac{e^2}{h\nu}\Big[{\sum_{\gamma\delta}}' A^\alpha_{\gamma\delta}A^\beta_{\delta\gamma} \mp \delta_{\varepsilon_1,\varepsilon_2}\left(A^\alpha_{12}A^\beta_{21} + A^\alpha_{21}A^\beta_{12}\right)\Big], \tag{13}$$

where $\sum'_{\gamma\delta}$ denotes the sum over $\gamma = 1, 2$ and all $\delta \neq \gamma$, and the upper (lower) sign refers again to triplets (singlets). Physically, the autocorrelator $S_{\alpha\alpha}$ is the shot noise measured in lead α.

Formula (13) can now be applied to the setting shown in figure 3, i.e., involving four leads and described by the single-particle scattering matrix elements, $s_{31} = s_{42} = r$, and $s_{41} = s_{32} = t$, where r and t denote the reflection and transmission amplitudes at the beam splitter. If we neglect backscattering (see section 2.7 for a discussion of the influence of

backscattering), i.e., $s_{12} = s_{34} = s_{\alpha\alpha} = 0$, then the noise correlations for the incident state $|\Psi_\pm\rangle$ are found to be (Burkard *et al* 2000)

$$S_{33} = S_{44} = -S_{34} = 2\frac{e^2}{h\nu} T\,(1-T)\left(1 \mp \delta_{\varepsilon_1\varepsilon_2}\right), \tag{14}$$

with $T = |t|^2$ the transmittivity of the beam splitter. One can check that for the remaining two triplet states $|\uparrow\uparrow\rangle$ and $|\downarrow\downarrow\rangle$ one also obtains equation (14) with the upper sign. As anticipated, the average current in all leads is a constant, both for singlets and triplets, $|\langle I_\alpha\rangle| = e/h\nu$. The shot noise power is often expressed in terms of the noise-to-current ratio (or, more accurately, the ratio between the actual noise power and that of a Poissonian source (Blanter and Büttiker 2000)), the so-called Fano factor, $F = S_{\alpha\alpha}/2e\,|\langle I_\alpha\rangle|$. In our case, the theoretical prediction for the Fano factor is (note the absence of a factor of $2e$ with the above definition of the Fano factor)

$$F = T(1-T)\left(1 \mp \delta_{\varepsilon_1\varepsilon_2}\right). \tag{15}$$

Formula (15) implies that if electrons in the singlet state $|\Psi_-\rangle$ with equal energies, $\varepsilon_1 = \varepsilon_2$, i.e., in the same orbital mode, are injected pairwise into the leads 1 and 2, then the zero frequency noise is *enhanced* by a factor of two (Burkard *et al* 2000), $F = 2T(1-T)$, with respect to the noise power for unentangled (uncorrelated) electrons (Büttiker 1990, 1992, Khlus 1987, Landauer 1989, Lesovik 1989, Martin and Landauer 1992), $F = T(1-T)$. As explained above, this noise enhancement is due to *bunching* of electrons in the outgoing leads, caused by the symmetric orbital wavefunction of the spin singlet $|S\rangle = |\Psi_-\rangle$. The triplet states $|T_0\rangle = |\Psi_+\rangle$, $|\uparrow\uparrow\rangle$, and $|\downarrow\downarrow\rangle$ exhibit *antibunching*, i.e. a complete suppression of the noise, $S_{\alpha\alpha} = 0$. The noise enhancement for the singlet $|\Psi_-\rangle$ is therefore a unique signature for entanglement (no unentangled state exists which can lead to the same signal). Entanglement can thus be observed by measuring the noise power of a mesoscopic conductor in a setup like figure 3. Distinguishing the triplet states $|\Psi_+\rangle$, $|\uparrow\uparrow\rangle$, and $|\downarrow\downarrow\rangle$ is not possible with the described noise measurement alone; their discrimination requires a measurement of the spins of the outgoing electrons, e.g. by using spin-selective tunnelling devices (Prinz 1998) into leads 3 and 4. However, as we shall discuss in section 2.6 below, there are ways to detect triplet entanglement if a local spin rotation mechanism (e.g., provided by the spin–orbit interaction) is available in at least one of the ingoing leads.

Signatures of entanglement in the charge transport statistics have also been formulated in the framework of the full counting statistics (Börlin *et al* 2002, Di Lorenzo and Nazarov 2005, Faoro *et al* 2004, Taddei *et al* 2005, Taddei and Fazio 2002). The generalization (for both bosons and fermions) to many particles interfering at a multi-port beam splitter is discussed in Lim and Beige (2005).

2.4. Leads with many modes

In our discussion so far, we have assumed that the leads that carry the spin-entangled electrons from the entangler to the beam splitter only conduct electrons via a single quantized mode. This has been extended to the continuum limit for the lead spectrum in Samuelsson *et al* (2004). We will follow a somewhat more general discussion (including the continuum case) for leads with multiple modes as presented in Egues *et al* (2005). In this general discussion, the parameter regimes in which singlet spin entanglement can be detected in the shot noise at a beam splitter (as discussed in section 2.3 above) have been identified. It turns out that even in the case where the entangled electrons are injected into a multitude of discrete states of the lead, we can observe two-particle coherence, and thus particle bunching and antibunching, and thus detect entangled states. In our discussion, we are not considering the possibility that, in a multi-mode

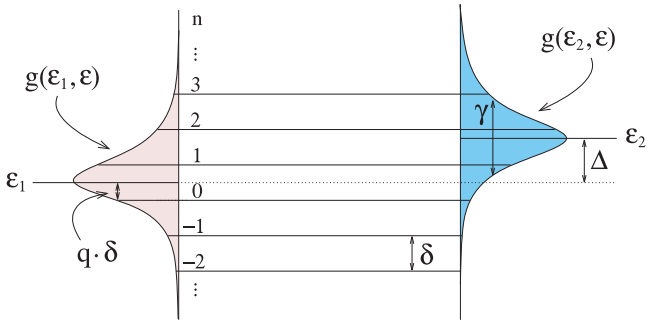

Figure 4. Energy diagram for the injection of entangled electrons into leads with multiple levels (Egues *et al* 2005). In the model discussed in the main text, the energy levels in the leads $n = 0, \pm 1, \pm 2, \ldots$ are assumed to be equidistant with spacing δ. The injection of electrons takes place at the mean energies $\varepsilon_{1,2}$ (for electron 1 and 2, respectively), separated by $\Delta = \varepsilon_2 - \varepsilon_1$, and with distributions $g(\varepsilon_{1,2}, \varepsilon)$ of width γ. Here, the distributions $g(\varepsilon_{1,2}, \varepsilon)$ are not drawn to scale, since their normalizations depend on the value of q.

setting, the two injected electrons can also be entangled in their orbital degrees of freedom. This possibility and its consequences for the entanglement detection via a noise measurement at a beam splitter have been investigated in Giovannetti *et al* (2006).

For our purposes, we first identify the relevant energy scales for the transport through multiple modes. These are the level spacing δ in the leads, the energy mismatch Δ of the injected electrons, and the energy broadening γ of the injected electrons (see figure 4). The relative magnitude of these three energies determine six different parameter regimes. In four of the six regimes, the full two-particle interference (and thus detection of spin entanglement) can be achieved asymptotically. In the two remaining parameter regimes, characterized by $\Delta \gg \delta, \gamma$, i.e., the energy mismatch exceeding both the level spacing and the energy broadening, we obtain no two-particle interference (these represent two distinct parameter regimes, since δ can be smaller or larger than γ).

The lead spectrum is assumed to consist of equidistant levels, i.e., $\varepsilon_n = n\delta + q\delta$, where $n = 0, \pm 1, \pm 2, \ldots$ and $0 \leqslant q < 1$ is some fixed offset. The injection of an electron with spin $\sigma = \uparrow, \downarrow$ into the lead α with energy distribution $g(\varepsilon, \varepsilon_n)$ centred at ε_n is now described by the creation operator

$$c^\dagger_{\alpha\sigma}(\varepsilon) = \sum_{n=-\infty}^{\infty} g(\varepsilon, \varepsilon_n) a^\dagger_{\alpha\sigma}(\varepsilon_n), \tag{16}$$

where $a^\dagger_{\alpha\sigma}(\varepsilon_n)$ creates an electron with the sharp energy ε_n as in equation (8). For the weight function g, we use the Breit–Wigner form

$$g(\varepsilon, \varepsilon') = \frac{g_0(\varepsilon)}{\varepsilon - \varepsilon' + \mathrm{i}\gamma}, \tag{17}$$

subject to the normalization condition $\sum_{n=-\infty}^{\infty} |g(\varepsilon, \varepsilon')|^2 = 1$.

Here, we assume that the entangler injects an electron with total probability 1, but with uncertain energy (e.g., using time-dependent tunnel barriers). This is different from the weak tunnelling case, e.g., from a quantum dot (Recher *et al* 2001). Analogous to equation (8), the spin-entangled singlet (−) and triplet (+) states for many-mode leads can be written with the new creation operators as

$$|\Psi_\pm\rangle = \frac{1}{\sqrt{2}} \left(c^\dagger_{1\uparrow}(\varepsilon_1) c^\dagger_{2\downarrow}(\varepsilon_2) \pm c^\dagger_{1\downarrow}(\varepsilon_1) c^\dagger_{2\uparrow}(\varepsilon_2) \right) |\psi_0\rangle. \tag{18}$$

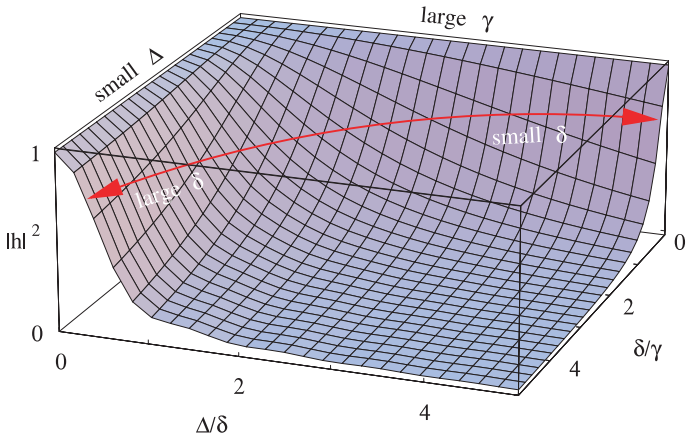

Figure 5. The two-particle interference visibility $|h(\Delta, \delta, \gamma)|^2$ from equation (22), plotted as a function of the dimensionless quantities Δ/δ and δ/γ, where $\Delta = \varepsilon_2 - \varepsilon_1$ denotes the mean energy difference between the two injected electrons, γ the width of their energy distributions, and δ the level spacing in the leads (see figure 4). The special case of matching energies $\varepsilon_1 \approx \varepsilon_2$ or $\Delta \ll \delta, \gamma$ corresponds to the edge labelled by 'small Δ'; here we find $|h|^2 = 1$, irrespective of the ratio γ/δ. The case of a broad energy distribution (fast injection) $\gamma \gg \Delta, \delta$ corresponds to the edge labelled 'large γ'; along this edge $|h|^2 = 1$, regardless of Δ/δ. A line of constant γ and Δ with variable δ is indicated by an arrow. For large δ, we find again $|h|^2 = 1$ for all Δ/γ, whereas for small δ (continuum limit), the limit $|h|^2 = 0$ or $|h|^2 = 1$ is reached, depending on whether $\Delta/\gamma \gg 1$ or $\Delta/\gamma \ll 1$.

The relation (16) allows us to express these states as

$$|\Psi_\pm\rangle = \sum_{\varepsilon_1', \varepsilon_2'} g(\varepsilon_1, \varepsilon_1') g(\varepsilon_2, \varepsilon_2') |\Psi_\pm\rangle_{\varepsilon_1', \varepsilon_2'}, \tag{19}$$

where $|\Psi_\pm\rangle_{\varepsilon_1', \varepsilon_2'}$ are the states with sharp energies, defined in equation (8). The normalization condition for $g(\varepsilon_1, \varepsilon_1')$ ensures that the average current in the outgoing leads of the beam splitter is unaffected by the spread in energy, i.e., $I_3 = I_4 = -e/h\nu$. However, the Fano factor $F = S_{33}/2eI_3$ does depend on the energy distribution,

$$F = T(1-T)\left(1 \mp |h(\varepsilon_1, \varepsilon_2)|^2\right), \tag{20}$$

where the upper (lower) sign corresponds to the entangled triplet (singlet), and where the overlap function h is defined as

$$h(\varepsilon_1, \varepsilon_2) = \sum_{\varepsilon} g(\varepsilon_2, \varepsilon)^* g(\varepsilon_1, \varepsilon). \tag{21}$$

For equidistant levels, this function has been evaluated exactly (note that the q dependence has dropped out),

$$|h|^2 = \frac{\gamma^2}{(\Delta/2)^2 + \gamma^2} \frac{\cosh^2(2\pi\gamma/\delta) - \cos^2(\pi\Delta/\delta)}{\sinh^2(2\pi\gamma/\delta)}. \tag{22}$$

In the case of injection into a single level, the $|h|^2$ term that appears in equation (20) for the Fano factor reduces to a Kronecker delta, as in equation (15). The role of the function $0 < |h(\Delta, \delta, \gamma)|^2 \leqslant 1$ is to quantify the visibility of two-particle interference. We plot the dimensionless quantity $|h(\Delta, \delta, \gamma)|^2$ as a function of the dimensionless ratios Δ/δ and δ/γ in figure 5. For maximal visibility, $|h|^2 = 1$, full bunching and antibunching of singlets and entangled triplets can be expected; this is the ideal case with regards to the detection of

entanglement. In the opposite case, $|h|^2 = 0$, bunching or antibunching cannot be observed at all because the two wave packets centred around ε_1 and ε_2 do not overlap in energy.

We briefly highlight the main parameter regimes (see also figure 5). (1) If the two electrons are injected with energy distributions whose centers coincide, $\Delta = \varepsilon_1 - \varepsilon_2 = 0$, then the interference is always maximal, $|h|^2 = 1$, irrespective of the values of the parameters δ and γ. For finite but small Δ, i.e., $\Delta \ll \gamma, \delta$, one finds $|h|^2 = 1 - \mathrm{O}(\Delta^2)$. More precisely, for $\Delta \ll \gamma \ll \delta$, the correction is $|h|^2 \simeq 1 - \pi^2\Delta^2/3\delta^2$, whereas for $\Delta \ll \delta \ll \gamma$, one finds $|h|^2 \simeq 1 - \Delta^2/4\gamma^2$. (2) If the energy broadening is small, $\gamma \ll \delta, \Delta$, then equation (22) yields

$$|h|^2 = \frac{\delta^2}{\pi^2\Delta^2}\sin^2\pi\frac{\Delta}{\delta} + \mathrm{O}(\gamma^2). \tag{23}$$

Here, the ratio δ/Δ is essential: if $\gamma \ll \delta \ll \Delta$ then the two electrons are injected into two different discrete states; therefore $|h|^2 \to 0$. In the opposite limit, $\gamma \ll \Delta \ll \delta$, the two electrons are injected into the same discrete level and $|h|^2 = 1 - \pi^2\Delta^2/3\delta^2 + \mathrm{O}(\Delta^4/\delta^4, \gamma^2)$. (3) The continuum limit is reached when $\delta \ll \Delta, \gamma$. In this case $|h|^2$ has the shape of a Lorentzian (Samuelsson *et al* 2004),

$$|h|^2 \simeq \frac{\gamma^2}{(\Delta/2)^2 + \gamma^2}. \tag{24}$$

Depending on the ratio γ/Δ, the two-particle interference is present or absent, i.e., $|h|^2 \to 0$ for $\delta \ll \gamma \ll \Delta$, while $|h|^2 \to 1$ for $\delta \ll \Delta \ll \gamma$. In summary, highly visible two-particle interference (and thus bunching and antibunching) $|h|^2 \to 1$ can be expected in all asymptotic regimes except for the detuned cases, $\Delta \gg \delta, \gamma$, where $|h|^2 \to 0$.

2.5. Lower bounds for entanglement

In section 2.3 above, the current fluctuations for a maximally entangled state (the singlet) have been discussed. Here, we extend this analysis to non-maximally entangled states. Such states can be both pure or mixed, and therefore are generally described by a density matrix χ. It turns out (Burkard and Loss 2003) that by using the zero-frequency noise amplitude after passage through the beam splitter (figure 6), one can determine a *lower bound* for the *amount* E of spin entanglement carried by individual pairs of electrons. One can therefore relate experimentally accessible quantities with a standard measure for entanglement, the entanglement of formation E (Bennett *et al* 1996b). Such knowledge is important since E quantifies the usefulness of a bipartite state for quantum communication.

We start our discussion from a general mixed state which we write in the singlet–triplet basis,

$$\chi = F_\mathrm{S}|\Psi_-\rangle\langle\Psi_-| + G_0|\Psi_+\rangle\langle\Psi_+| + \sum_{i=\uparrow,\downarrow} G_i|ii\rangle\langle ii| + \Delta\chi, \tag{25}$$

where $\Delta\chi$ denotes off-diagonal terms. The singlet fidelity F_S quantifies the probability that the electron pair is in a spin-singlet state (we use the subscript S here in order to distinguish the singlet fidelity from the Fano factor; in the literature, F is often used for F_S). Next, one can decompose the current correlators equation (12) as

$$S_{\alpha\beta} \equiv S^\chi_{\alpha\beta} = F_\mathrm{S}S^{|\Psi_-\rangle}_{\alpha\beta} + G_0 S^{|\Psi_+\rangle}_{\alpha\beta} + \sum_{i=\uparrow,\downarrow} G_i S^{|ii\rangle}_{\alpha\beta}, \tag{26}$$

where we have defined $S^{|\Psi\rangle}_{\alpha\beta} \equiv S^{|\Psi\rangle\langle\Psi|}_{\alpha\beta}$. The off-diagonal terms in $\Delta\chi$ need not be specified further, as they do not enter $S_{\alpha\beta}$ due to the spin-conserving nature of the operators $\delta I_\alpha(t)$. The

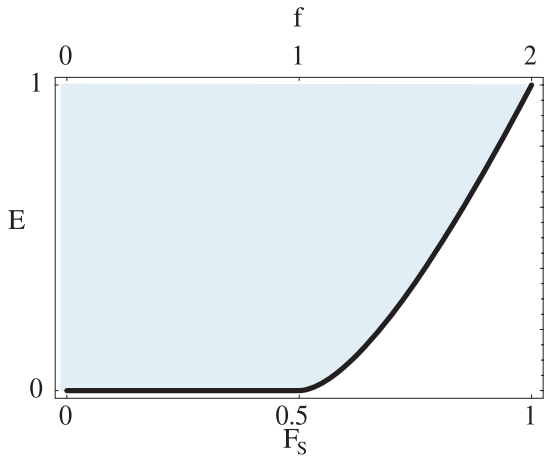

Figure 6. Entanglement of formation E of the electron spins as a function of the singlet fidelity F_S and the reduced correlator $f = S_{33}/2eIT(1-T) = 2F_S$. The points on the curve represent the exact relation for Werner states, the shaded (blue) area above the curve represents general states, for which the curve is a lower bound of E. Possible values of E and f (or F_S) are in the shaded region.

prefactors F_S, G_0, $G_\uparrow$, and $G_\downarrow$ are the diagonal matrix elements of χ and are determined by the state preparation, i.e., the entangler.

In section 2.3 we showed that the singlet state $|S\rangle = |\Psi_-\rangle$ gives rise to enhanced shot noise (and cross-correlators), $S_{33}^{|\Psi_-\rangle} = -S_{34}^{|\Psi_-\rangle} = 2eIT(1-T)f$, with the *reduced correlator* $f = 2$, as compared to the 'classical' Poissonian value $f = 1$. The spin-triplet states, on the other hand, are noiseless, $S_{\alpha\beta}^{|\Psi_+\rangle} = S_{\alpha\beta}^{|\uparrow\uparrow\rangle} = S_{\alpha\beta}^{|\downarrow\downarrow\rangle} = 0$ ($\alpha, \beta = 3, 4$). Therefore, both the auto- and cross-correlations are only due to the singlet component of the incident two-particle state,

$$S_{33} = -S_{34} = F_S S^{|\Psi_-\rangle} = 2eIT(1-T)f, \tag{27}$$

where $f = 2F_S$. So, a noise measurement simply provides us with the information about the singlet fraction of the state. This already suggests that, in general, we cannot expect to get full information about the entanglement E of the state, since E is a function of the entire density matrix χ of which we know only one matrix element! From this point of view it is astonishing how much we can know about the entanglement E by knowing only F_S: as we explain below, we can always obtain a lower bound on E which becomes tight if the state is a singlet ($F_S = 1$, $E = 1$) or any other spherically symmetric state.

Given a *pure* bipartite state, $|\psi\rangle \in \mathcal{H}_A \otimes \mathcal{H}_B$, we can use the von Neumann entropy $S_N(|\psi\rangle) = -\mathrm{Tr}_B\, \rho_B \log \rho_B$ (log in base 2) of the reduced density matrix $\rho_B = \mathrm{Tr}_A\, |\psi\rangle\langle\psi|$, to quantify the entanglement. This quantity is always between 0 and 1, $0 \leqslant S_N \leqslant 1$, and is maximal for the Bell states, $S_N(|\Psi_\pm\rangle) = S_N(|\Phi_\pm\rangle) = 1$. If it vanishes, then the state is unentangled (i.e., a tensor product state), $S_N(|\psi\rangle) = 0 \Leftrightarrow |\psi\rangle = |\psi\rangle_A \otimes |\psi\rangle_B$. The operational meaning is that if $S_N(|\psi\rangle) \simeq N/M$ then $M \geqslant N$ copies of $|\psi\rangle$ are sufficient to perform, e.g., quantum teleportation of N qubits for $N, M \gg 1$ (and similarly for other quantum communication protocols). Entanglement measures also exist for *mixed* states. The entanglement of formation of a bipartite state χ (Bennett *et al* 1996b) is defined as $E(\chi) = \min_{\{(|\chi_i\rangle, p_i)\} \in \mathcal{E}(\chi)} \sum_i p_i S_N(|\chi_i\rangle)$, where $\mathcal{E}(\chi) = \{(|\chi_i\rangle, p_i) | \sum_i p_i |\chi_i\rangle\langle\chi_i| = \chi\}$ is the set of possible decompositions of the density matrix into ensembles of pure states. Therefore, E is the smallest averaged entanglement of any ensemble of pure states realizing χ. In an operational sense, $E(\chi)$ measures the number of EPR pairs (asymptotically, averaged over

many copies) required to form one copy of the state χ. A state with $E > 0$ is entangled (a state with $E = 1$ is maximally entangled and thus pure), and neither local operations nor classical communication (LOCC) between A and B can increase E.

Given an arbitrary mixed state of two qubits χ, it is known that $E(\chi)$ is a relatively complicated function of χ (Wootters 1998). In particular, it is in general certainly not a function of the singlet fidelity $F_S = \langle\Psi_-|\chi|\Psi_-\rangle$ alone. For the subclass of spherically symmetric states, however, the entanglement only depends on F_S, i.e., $E(\chi) = E(F_S)$. These states, known as Werner states (Werner 1989), have the form

$$\rho_{F_S} = F_S|\Psi_-\rangle\langle\Psi_-| + \frac{1-F_S}{3}\left(|\Psi_+\rangle\langle\Psi_+| + |\Phi_-\rangle\langle\Phi_-| + |\Phi_+\rangle\langle\Phi_+|\right). \tag{28}$$

There is an explicit analytic expression for the entanglement of formation of the Werner states (Bennett *et al* 1996b):

$$E(F_S) \equiv E(\rho_{F_S}) = \begin{cases} H_2\left(1/2 + \sqrt{F_S(1-F_S)}\right) & \text{if } 1/2 < F_S \leqslant 1, \\ 0 & \text{if } 0 \leqslant F_S < 1/2, \end{cases} \tag{29}$$

where we have used the dyadic Shannon entropy $H_2(x) = -x\log x - (1-x)\log(1-x)$. Combining equation (29) with equation (27), one can express $E(\rho_{F_S})$ in terms of the (reduced) shot noise power f. The relation between $E(\rho_{F_S})$ and F_S (resp., f) is plotted in figure 6.

Using the expression for the entanglement of formation of Werner states, we can derive a lower bound on the entanglement of arbitrary mixed states χ with the following argument. An arbitrary mixed state χ can be transformed into a spherical symmetric state ρ_{F_S} with $F_S = \langle\Psi_-|\chi|\Psi_-\rangle$ by a random bipartite rotation ('twirl') (Bennett *et al* 1996a, 1996b), i.e. by applying $U \otimes U$ with a random $U \in SU(2)$. Because the twirl is a local (LOCC) operation, entanglement can only decrease (or remain constant) under the twirl,

$$E(F_S) \leqslant E(\chi). \tag{30}$$

As a consequence, the entanglement of formation $E(F_S)$ of the associated Werner state (with same singlet fidelity F_S) is a *lower bound* on $E(\chi)$ (figure 6). If the noise power exceeds a certain value, $f = 2F_S > 1$, in the beam splitter setup figure 3 then we know that it must be due to entanglement between the electron spins injected into leads 1 and 2, i.e., $E(F_S) > 0$.

2.6. Use of spin–orbit coupling

The lower bound from section 2.5 is useful if one is assessing a source that produces spin-singlet entanglement. An extension to arbitrary entangled states is possible if a means of rotating the spin of the carriers in one of the ingoing arms of the beam splitter is available (Burkard and Loss 2003, Egues *et al* 2002).

It has been proposed to use the Rashba spin–orbit coupling in order to implement such single-spin rotations in one of the leads going into the beam splitter (Egues *et al* 2002). This analysis has been extended to up to two bands with both Rashba and Dresselhaus spin–orbit coupling present (Egues *et al* 2005).

We restrict ourselves here to the Rashba spin–orbit coupling and a single mode of the lead, to make the discussion as simple as possible. The Rashba spin–orbit coupling in, say, lead 1, has the effect of rotating the spin injected in lead 1 by some angle θ_R. This can be taken into account by multiplying the rotation matrix

$$U_R = \begin{pmatrix} \cos\theta_R/2 & -\sin\theta_R/2 \\ \sin\theta_R/2 & \cos\theta_R/2 \end{pmatrix} \tag{31}$$

from the right with the scattering matrix blocks that involve lead 1; $s^{\mathrm{R}}_{31} = s_{31}U_{\mathrm{R}}$ and $s^{\mathrm{R}}_{41} = s_{41}U_{\mathrm{R}}$. This rotates within the (entangled) singlet–triplet space, and yields the Fano factor

$$F = T(1-T)(1 \mp \cos\theta_{\mathrm{R}}\delta_{\varepsilon\varepsilon'}); \tag{32}$$

thus the classical inequality ($F \leqslant 1$) can be violated for both the singlet and the entangled triplet by sweeping the Rashba angle θ_{R}, while all unentangled triplet states still yield $F \leqslant 1$. Therefore, the Rashba rotation allows for the detection of entangled triplets in addition to the singlet. Similarly, spin rotations about an arbitrary axis allow the detection of all entangled states (in particular, all Bell states) with noise measurements.

2.7. Backscattering

Imperfections in the leads and the beam splitter can lead to undesired scattering of electrons back into the same lead, or, e.g., from lead 1 to 2. Noisy injection from the entangler can be treated on the same footing as backscattering in the leads. In our discussion above, such backscattering processes has been neglected. Backscattering is a noise source which is unrelated to entanglement. Thus, it is important to ask whether there is a danger of a 'false positive', i.e., a noise signal that could be interpreted as entanglement although it really originates from backscattering. This problem has been analysed for a symmetric beam splitter in Burkard and Loss (2003), and in more detail in Egues *et al* (2005), where also the asymmetric backscattering of local Rashba spin–orbit interaction in one of the leads was analysed. The effect of inelastic backscattering (which we will not discuss here) has also been analysed (San-Jose and Prada 2006).

For symmetric backscattering with total backscattering probability R_{B}, one obtains (Burkard and Loss 2003)

$$S_{33} = 2eI\left[2F_{\mathrm{S}}(1-R_{\mathrm{B}})T(1-T) + R_{\mathrm{B}}/2\right], \tag{33}$$

and similarly for the cross-correlations S_{34}, where the first term is the shot noise due to the (entangled) singlet fidelity F_{S} of the state, reduced by the backscattering factor $1 - R_{\mathrm{B}}$, while the second term is the noise generated by the backscattering itself. As expected, equation (33) reduces to equation (14) for $R_{\mathrm{B}} = 0$. As long as $R_{\mathrm{B}} > 1/2$, one can still obtain a useful lower bound for entanglement (see section 2.5) even if R_{B} is not known precisely. If R_{B} is known, e.g., from measurements of the average current, then the backscattering effects can be taken into account and do not affect the quality of entanglement detection. Similar results apply for the backscattering due to spin–orbit coupling in one of the leads (Egues *et al* 2005).

2.8. Bell's inequalities

Although they may be very challenging to do in practice (see above), direct tests of Bell's inequalities (Bell 1966, Mermin 1993) or related inequalities by Clauser and Horne (1974) with spin-entangled electrons using spin-sensitive detectors have been proposed by several authors (Kawabata 2001, Maître *et al* 2000). In contrast to the charge detection in sections 2.3 and 2.5, this task involves the measurement of a spin current. Combinations of the Andreev entangler (see below) setup with a Bell test were studied in Chtchelkatchev *et al* (2002), Samuelsson *et al* (2003). The possibility of a violation of the Clauser–Horne inequality in the full-counting statistics has been predicted in Prada *et al* (2005). As an alternative to standard Bell tests, it has been proposed to use so-called entanglement witnesses (Blaauboer and DiVincenzo 2005).

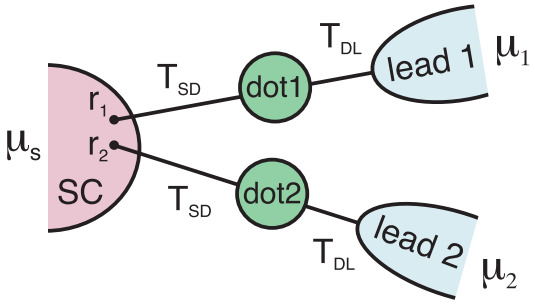

Figure 7. Schematic diagram of the Andreev entangler as proposed in Recher *et al* (2001). Andreev tunnelling takes place as follows: a Cooper pair in the superconductor (SC) is separated into two spin-entangled electrons which tunnel with amplitude T_{SD} from two points $\mathbf{r}_1, \mathbf{r}_2$ of the SC onto the two quantum dots 1 and 2. The dots are coupled to normal leads 1 and 2 with tunnelling amplitude T_{DL}. The entangler will be most efficient for asymmetric barriers, $|T_{SD}|/|T_{DL}| \ll 1$.

3. Production of spin entanglement

3.1. Superconductor–normal junctions

The condensate in a conventional superconductor (SC) with s-wave pairing symmetry consists of a large number of Cooper pairs that are in the spin-singlet state, equation (1). A device that harnesses this large reservoir of entangled singlets has been proposed in Recher *et al* (2001): it consists of an SC contact (at the chemical potential μ_S) from which quantum tunnelling of single electrons to two quantum dots is possible with a quantum amplitude T_{SD}. The quantum dots, in turn, are coupled with tunnelling amplitude T_{DL} to the normal leads L_1 and L_2 (both at the chemical potential $\mu_1 = \mu_2$); see figure 7.

The desired physical process for entanglement generation is Andreev tunnelling, where two electrons (one with spin up and another one with spin down) tunnel coherently through a normal barrier (Hekking *et al* 1993). At the same time, single-particle tunnelling is suppressed by the presence of the intermediate quantum dots, forcing the two electrons from a Cooper pair to tunnel coherently into *separate* leads rather than both into the same lead. The double occupation of a quantum dot is suppressed by the Coulomb blockade mechanism (Kouwenhoven *et al* 1997). The transport of entangled electrons from the SC to the quantum dots and from there to the normal leads can be controlled with an applied bias voltage $\Delta\mu = \mu_S - \mu_l > 0$ $(l = 1, 2)$.

The parameter regime for the generation of spin-entangled electrons is discussed in Recher *et al* (2001): the barriers of the quantum dots need to be asymmetric, $|T_{SD}| \ll |T_{DL}|$, the temperature must be sufficiently small, $\Delta\mu > k_B T$, and $\Delta, U, \delta\epsilon > \Delta\mu > \gamma_l, k_B T$, and $\gamma_l > \gamma_S$, where Δ is the SC energy gap, $\delta\epsilon$ is the single-level spacing of the dots, and $\gamma_l = 2\pi\nu_l|T_{SD}|^2$ are the tunnelling rates from lead l to the quantum dot (and vice versa). The quality of the device is characterized by the ratio between the current I_1 of pairwise entangled electrons tunnelling into different leads and the leakage current I_2 of electron pairs that end up in the same lead (Recher *et al* 2001),

$$\frac{I_1}{I_2} = \frac{2\mathcal{E}^2}{\gamma^2}\left[\frac{\sin(k_F\delta r)}{k_F\delta r}\right]^2 e^{-2\delta r/\pi\xi}, \tag{34}$$

$$\frac{1}{\mathcal{E}} = \frac{1}{\pi\Delta} + \frac{1}{U}. \tag{35}$$

Here, k_F denotes the Fermi wavevector, $\gamma = \gamma_1 + \gamma_2$, and ξ the SC coherence length.

The desired current I_1 decreases exponentially with increasing distance $\delta r = |\mathbf{r}_1 - \mathbf{r}_2|$ between the tunnelling points on the SC, the scale given by the superconducting coherence length ξ. With ξ typically being on the order of μm, this does not pose severe restrictions for a conventional s-wave SC. In the important case $0 \leqslant \delta r \sim \xi$ the suppression is only polynomial $\propto 1/(k_F\delta r)^2$, with k_F being the Fermi wavevector in the SC. One also observes that the effect of the quantum dots consists in the suppression factor $(\gamma/\mathcal{E})^2$ for tunnelling into the same lead. One therefore has to impose the additional condition $k_F\delta r < \mathcal{E}/\gamma$, which can be satisfied for small dots with $\mathcal{E}/\gamma \approx 100$ and $k_F^{-1} \approx 1$ Å.

Electron entangler devices with an SC reservoir attached to normal leads have also been investigated in Lesovik *et al* (2001), Prada and Sols (2004), Sauret *et al* (2004). The presence of voltage noise on the two quantum dots can lead to a reduction of the ratio (34), as analysed in Dupont and Le Hur (2006).

Shot noise and conductance measurements have been achieved in a quasi-ballistic SC–normal beam-splitter junction (Choi *et al* 2005). Moreover, transport properties of structures with an SC lead attached to normal leads have been studied experimentally (Russo *et al* 2005).

3.2. Superconductor–Luttinger-liquid junctions

The production of electron spin entanglement requires interaction between the electrons; in the case discussed in the previous section 3.1, the repulsive Coulomb interaction in the quantum dots attached to the SC reservoir is used to separate the two entangled electrons. Alternatively, a resistive lead where the dynamical Coulomb blockade effect helps to separate the electron pair has been proposed (Recher and Loss 2003).

A strongly interacting electron system in one spatial dimension can be described as a Luttinger liquid (Tsvelik 2003). A Luttinger liquid opens another possibility to separate entangled electrons from an SC (Bena *et al* 2002, Recher and Loss 2002a, 2002b). Physical systems with Luttinger-liquid behaviour are, for example, metallic carbon nanotubes (Egger and Gogolin 1997, Kane *et al* 1997). The setup studied theoretically in Recher and Loss (2002a, 2002b) is composed of two separate one-dimensional conductors (e.g., carbon nanotubes), each forming a Luttinger liquid, which are tunnel-coupled (at a point far from their ends) to an SC; see figure 8. The two wires are assumed to be sufficiently separated, such that interactions between carriers in different wires can be neglected.

The fundamental excitations of a Luttinger liquid (if backscattering is absent) are long-wavelength charge and spin density waves propagating with velocities $u_\rho = v_F/K_\rho$ (charge) and $u_\sigma = v_F$ (spin) (Schulz 1990), with v_F the Fermi velocity and $K_\rho < 1$ for an interacting system. The tunnelling of electrons from the SC to the one-dimensional (Luttinger liquid) wires is modelled by the Hamiltonian

$$H_T = t_0 \sum_{ns} \psi_{ns}^\dagger \Psi_s(\mathbf{r}_n) + \text{H.c.}, \tag{36}$$

where $\Psi_s(\mathbf{r}_n)$ is the annihilation (field) operator for an electron with spin s at the location $\mathbf{r}_n$ in the SC nearest to the one-dimensional wire $n = 1, 2$, and $\psi_{ns}^\dagger$ is the operator that creates an electron at the coordinate x_n in the wire n. Applying a bias $\mu = \mu_S - \mu_l$ between the SC (with chemical potential μ_S) and the leads (μ_l) induces the flow of a stationary current of pairwise spin-entangled electrons from the SC to the one-dimensional wires.

Similar to the case of the Andreev entangler with attached quantum dots, discussed in section 3.1 above, the performance of this device can be quantified by the ratio between the

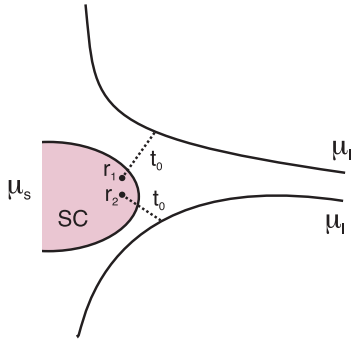

Figure 8. The entangler as proposed in Recher and Loss (2002a, 2002b), with a superconductor (SC) tunnel-coupled to two one-dimensional wires at positions $\mathbf{r}_1$ and $\mathbf{r}_2$ on the SC with tunnelling amplitude t_0.

two competing currents, I_1 for electrons tunnelling into separate leads, thus contributing to entanglement between the remote parts of the system, and I_2 for electrons tunnelling into the same lead, thus not contributing to entanglement. From a T-matrix calculation (Recher and Loss 2002a, 2002b), one obtains in leading order in μ/Δ, where Δ denotes the SC excitation gap, and at zero temperature,

$$I_1 = \frac{I_1^0}{\Gamma(2\gamma_\rho + 2)} \frac{v_F}{u_\rho} \left[\frac{2\Lambda\mu}{u_\rho}\right]^{2\gamma_\rho}, \tag{37}$$

$$I_1^0 = 4\pi e\gamma^2\mu \frac{\sin^2(k_F\delta r)}{(k_F\delta r)^2} e^{-2\delta r/\pi\xi}, \tag{38}$$

$$I_2 = I_1(\delta r \to 0) \sum_{b=\pm 1} A_b \left(\frac{2\mu}{\Delta}\right)^{2\gamma_{\rho b}}, \tag{39}$$

where Γ is the Gamma function, Λ a short-distance cut-off of the order of the lattice spacing in the Luttinger liquid, $\gamma = 2\pi\nu_S\nu_l|t_0|^2$ the probability per spin to tunnel from the SC to the one-dimensional leads, ν_S and ν_l the energy density of states per spin for the SC and the one-dimensional leads at the chemical potentials μ_S and μ_l, respectively, and δr the separation between the tunnelling points on the SC. The constant A_b is of order one and does not depend on the interaction strength. Furthermore, we have used the definitions $\gamma_{\rho+} = \gamma_\rho$ and $\gamma_{\rho-} = \gamma_{\rho+} + (1-K_\rho)/2 > \gamma_{\rho+}$. Note that in equation (39), the current I_1 needs to be evaluated at $\delta r = 0$. In the non-interacting limit, $I_2 = I_1 = I_1^0$ is obtained by putting $\gamma_\rho = \gamma_{\rho b} = 0$, and $u_\rho = v_F$.

In order to obtain a finite measurable current, the coherence length ξ of the Cooper pairs should exceed δr (as in section 3.1 for the Andreev entangler). It has been argued that the suppression of the current by $1/(k_F\delta r)^2$ can be considerably reduced by using low-dimensional SCs (Recher and Loss 2002a, 2002b). The undesired injection of two electrons into the same lead (current I_2) is suppressed compared to I_1 by a factor of $(2\mu/\Delta)^{2\gamma_{\rho+}}$, where $\gamma_{\rho+} = \gamma_\rho$, if the two electrons are injected into the same direction (left or right movers), or by $(2\mu/\Delta)^{2\gamma_{\rho-}}$ if they propagate in different directions. The first scenario (same direction) is the more likely one since $\gamma_{\rho-} > \gamma_{\rho+}$. The suppression of I_2 by $1/\Delta$ is due to the two-particle correlations in the Luttinger liquid when the electrons tunnel into the same lead, similar to the Coulomb blockade effect for tunnelling into quantum dots in the previous section 3.1. The delay time between the two electrons from the same Cooper pair is controlled by the inverse SC gap Δ^{-1}; i.e., if Δ becomes larger, the electrons arrive within a shorter time interval, thus increasing the

correlations and further suppressing the unwanted I_2. Increasing the bias μ has the opposite effect, since it opens up more available states into which the electron can tunnel, and therefore the effect of the SC gap Δ is mitigated.

Noise correlations in the current carried by the entangled electrons emitted by a carbon nanotube–SC entangler are studied in Bouchiat *et al* (2003).

3.3. Quantum dots coupled to normal leads

The Coulomb interaction between electrons in a quantum dot has also been suggested as the main mechanism in electron spin entanglers with normal (as opposed to SC) leads. Entanglers comprising a single quantum dot attached to special leads with a very narrow bandwidth (Oliver *et al* 2002) or with three coupled quantum dots (Saraga and Loss 2003) coupled to ordinary leads have been analysed. The idea behind both proposals is to extract the singlet ground state of a single quantum dot occupied by two electrons by moving the two electrons into two separate leads. In both proposals, the separation is enhanced due to two-particle energy conservation. Different ideas using double-dot turnstile devices with time-dependent barriers were followed in Blaauboer and DiVincenzo (2005), Hu and Das Sarma (2004).

3.4. Coulomb scattering in a 2D electron system

Motivated by scanning probe imaging and control of electron flow in a two-dimensional electron system in a semiconductor heterostructure (Topinka *et al* 2000, 2001), it has been proposed to use this technique to generate electron spin entanglement by controlling Coulomb scattering in a interacting 2D electron system (Saraga *et al* 2004, 2005). For a scattering angle of $\pi/2$, constructive two-particle interference is expected to lead to an enhancement of the spin-singlet scattering probability, and at the same time, a reduction of the triplet scattering. These scattering amplitudes (and probabilities) have been obtained using the Bethe–Salpeter equation for small r_s, which in turn allowed for an estimate of the achievable current of spin-entangled electrons (Saraga *et al* 2004, 2005).

3.5. Other spin entangler proposals

In Costa and Bose (2001), the use of a magnetic impurity in a special beam-splitter geometry was proposed for the purpose of generating spin entanglement between ballistic electrons in a two-dimensional electron system. The process where two magnetic impurities become entangled via electron scattering has been described more recently (Costa *et al* 2006).

The generation of entanglement using two-particle interference in combination with which-way detection (charge detection) has been discussed in Bose and Home (2002).

The use of a sole carbon nanotube to create spin entanglement between a localized and an itinerant electron has been suggested in Gunlycke *et al* (2006).

Entanglement between electrons subject to the spin–orbit interaction in a quantum dot, in the absence of interaction, has been discussed in Frustaglia *et al* (2006).

4. Transport of entangled electrons

An electron spin qubit does not travel 'on its own'—it is always attached to the electron's charge. This is an enormous advantage for many reasons, one being that spin information can be converted into charge information, which then allows sensitive read-out (Loss and DiVincenzo 1998). Another advantage, of interest in the present context, is that the charge responds to

externally applied fields and therefore electron spin qubits can in principle be transported in an electric conductor.

This has prompted the question whether a pair of entangled electron spins could be produced in one location on a semiconductor structure and subsequently distributed over some distance on-chip, to be consumed later for some quantum information task (see section 1.1). Such transport has certainly reached quite an advanced level for photon qubits, reaching distances of kilometres (Gisin *et al* 2002). Even for modest distances, perhaps micrometres, within, for example, a semiconductor structure, this is not straightforward for electrons. An electron that is injected into a metallic wire becomes immersed into a sea of other electrons that (i) are indistinguishable from the injected electron, and (ii) interact with all other electrons, including the injected one. Here, we report on the theoretical discussion regarding the stability of spin entanglement an interacting many-electron system (Burkard *et al* 2000, DiVincenzo and Loss 1999). To anticipate the main results, it turns out that the indistinguishability of particles is harmless for spin entanglement, whereas Coulomb interactions do affect entanglement, but only to some extent because the electron–electron interactions are typically screened (Mahan 1993). As discussed in more detail below, an electron being added to the a metallic wire in the orbital state q will be 'dressed' by the interactions on a very short time scale (inverse plasma frequency). The resulting state has a quasiparticle weight in state q which is renormalized by a factor z_f with $0 \leqslant z_q \leqslant 1$. The weight z_q quantifies how likely it is to find an electron in the original state q, while $1 - z_q$ is the part that is distributed among all the other states.

We can describe the time evolution of the entangled triplet or singlet states in the interacting many-electron system by introducing the two-particle Green's function

$$G^{\mathrm{t/s}}(\mathbf{12}, \mathbf{34}; t) = \left\langle \psi^{\mathrm{t/s}}_{\mathbf{12}}, t | \psi^{\mathrm{t/s}}_{\mathbf{34}} \right\rangle, \tag{40}$$

where we use the second-quantized notation introduced in equation (8) above. The singlet/triplet Green's function defined in equation (40) above can be expressed in terms of the standard two-particle Green's function (Mahan 1993) $G(12, 34; t)$ by

$$G^{\mathrm{t/s}}(\mathbf{12}, \mathbf{34}; t) = -\tfrac{1}{2} \sum_{\sigma} \left[G(1\bar{2}, 3\bar{4}; t) \pm G(1\bar{2}, \bar{3}4; t) \right], \tag{41}$$

where $n = (\mathbf{n}, \sigma)$ and $\bar{n} = (\mathbf{n}, -\sigma)$. The $+$ sign stands for the triplet (t), and the $-$ sign for the singlet (s) Green's function. If, at time $t = 0$, a spin-triplet (spin-singlet) state is prepared, then we can define the fidelity of transmission as the probability for finding a triplet (singlet) after time t,

$$P(t) = |G^{\mathrm{t/s}}(\mathbf{12}, \mathbf{12}; t)|^2. \tag{42}$$

To calculate the fidelity (42), we can therefore use equation (41) to reduce the problem to that of calculating the (standard) two-particle Green's function

$$G(12, 34; t) = -\left\langle T a_1(t) a_2(t) a_3^\dagger a_4^\dagger \right\rangle \tag{43}$$

for a time- and spin-independent Hamiltonian, $H = H_0 + \sum_{i<j} V_{ij}$, where H_0 describes the free motion of N electrons, and V_{ij} is the bare Coulomb interaction between electrons i and j, $\langle \cdots \rangle$ denotes the zero-temperature expectation value, and T is the time-ordering operator. In the case where the leads are sufficiently separated, the vertex part in $G(12, 34; t)$ vanishes, and thus the two-particle Green's function can be expressed in terms of interacting single-particle Green's functions $G(\mathbf{n}, t)$ via

$$G(12, 34; t) = G(13, t) G(24, t) - G(14, t) G(23, t), \tag{44}$$

where ($l = 1, 2$)

$$G(\mathbf{n}, t) = -\mathrm{i} \langle \psi_0 | T a_{\mathbf{n}}(t) a_{\mathbf{n}}^\dagger | \psi_0 \rangle \equiv G_l(\mathbf{q}, t). \tag{45}$$

For the singlet/triplet Green's functions, this leads, with equation (41), to

$$G^{\mathrm{t/s}}(\mathbf{12}, \mathbf{34}; t) = -G(\mathbf{1}, t)\, G(\mathbf{2}, t)[\delta_{\mathbf{13}}\delta_{\mathbf{24}} \mp \delta_{\mathbf{14}}\delta_{\mathbf{23}}]. \tag{46}$$

At $t = 0$ (or as long as interactions are absent) one finds $G(\mathbf{n}, t) = -\mathrm{i}$ and $G^{\mathrm{t/s}} = \delta_{\mathbf{13}}\delta_{\mathbf{24}} \mp \delta_{\mathbf{14}}\delta_{\mathbf{23}}$; the fidelity remains $P = 1$. Under the influence of interactions and for times $0 \leqslant t \lesssim 1/\Gamma_q$ shorter than the quasiparticle lifetime $1/\Gamma_q$, one can use the standard result for particle energies $\epsilon_q = q^2/2m$ near the Fermi energy ϵ_{F} (Mahan 1993),

$$G_{1,2}(\mathbf{q}, t) \approx -\mathrm{i}z_q\theta(\epsilon_q - \epsilon_{\mathrm{F}})\mathrm{e}^{-\mathrm{i}\epsilon_q t - \Gamma_q t}. \tag{47}$$

In a two-dimensional electron system (2DES), e.g. in a GaAs heterostructure, one finds $\Gamma_q \propto (\epsilon_q - \epsilon_{\mathrm{F}})^2 \log(\epsilon_q - \epsilon_{\mathrm{F}})$ (Giuliani and Quinn 1982) using the random phase approximation (RPA) to take into account the screening of the Coulomb interaction (Mahan 1993). It remains to evaluate the quasiparticle weight at the Fermi surface,

$$z_{\mathrm{F}} = \left(1 - \frac{\partial}{\partial\omega}\,\mathrm{Re}\,\Sigma_{\mathrm{ret}}(k_{\mathrm{F}}, \omega)\right)^{-1}\Bigg|_{\omega=0}, \tag{48}$$

where $\Sigma_{\mathrm{ret}}(q, \omega)$ is the retarded irreducible self-energy. The fidelity can then be expressed through z_{F} as

$$P = z_{\mathrm{F}}^4. \tag{49}$$

This can be seen by evaluating the two-particle Green's function for momenta $\mathbf{q}$ near the Fermi surface, assuming that the two leads that carry the two entangled particles are identical ($G_1 = G_2$). One finds $|G^{\mathrm{t/s}}(\mathbf{12}, \mathbf{34}; t)|^2 = z_{\mathrm{F}}^4\,|\,\delta_{\mathbf{13}}\delta_{\mathbf{24}} \mp \delta_{\mathbf{14}}\delta_{\mathbf{23}}|^2$, for sufficiently short times, $0 < t \lesssim 1/\Gamma_q$.

Finally, in order to evaluate the quasiparticle weight factor, equation (50), we need the irreducible self-energy Σ_{ret}. For a two-dimensional electron system (2DES), this quantity has been evaluated explicitly in leading order of the interaction parameter $r_s = 1/k_{\mathrm{F}}a_{\mathrm{B}}$, where $a_{\mathrm{B}} = \epsilon_0\hbar^2/me^2$ is the Bohr radius, (Burkard *et al* 2000, DiVincenzo and Loss 1999), with the result

$$z_{\mathrm{F}} = \frac{1}{1 + r_s\,(1/2 + 1/\pi)}. \tag{50}$$

This result has been extended to include corrections due to the Rashba spin–orbit interaction (Saraga and Loss 2005) and finite temperatures (Galitski and Sarma 2004). In a standard GaAs 2DES, one can estimate $a_{\mathrm{B}} = 10.3$ nm and $r_s = 0.614$, which yield a quasiparticle weight of $z_{\mathrm{F}} = 0.665$. Numerical evaluation of the RPA self-energy, summing up all orders of r_s within this approximation, yield the more accurate result $z_{\mathrm{F}} = 0.691$. Substituting z_{F} back into equation (49), we obtain approximately $P \approx 0.2$. For larger electron density, i.e., smaller r_s, one can expect P to be closer to one. It also needs to be stressed that P is a fidelity without postselection. Typically, it is sufficient to count only the fidelity of the postselected singlet pairs, i.e., those that can successfully be retrieved from the Fermi sea. This postselected fidelity is not affected by the (spin-independent) Coulomb interaction at all, i.e., $P_{\mathrm{postsel}} = 1$, provided that spin-scattering effects are negligible. The degree to which spin-scattering events are really negligible can be quantified from experiments that measure the spin coherence length (Awschalom and Kikkawa 1999, Kikkawa and Awschalom 1998, Kikkawa *et al* 1997). In these experiments, it was found that the spin coherence length can exceed 100 μm in GaAs 2DESs.

References

Aspect A, Dalibard J and Roger G 1982 *Phys. Rev. Lett.* **49** 1804
Averin D V and Nazarov Y V 1992 *Single Charge Tunneling* (*NATO ASI Series B: Physics* vol 294) ed H Grabert and M H Devoret (New York: Plenum)
Awschalom D D and Kikkawa J M 1999 *Phys. Today* **52** 33
Beenakker C W J 2006 *Proc. Int. School Phys. E. Fermi* vol 162 (Amsterdam: IOS Press) (*Preprint* cond-mat/9906071)
Bell J S 1966 *Rev. Mod. Phys.* **38** 447
Bena C, Vishveshwara S, Balents L and Fisher M P A 2002 *Phys. Rev. Lett.* **89** 037901
Bennett C H, Brassard G, Crépeau C, Jozsa R, Peres A and Wootters W K 1993 *Phys. Rev. Lett.* **70** 1895
Bennett C H, Brassard G, Popescu S, Schumacher B, Smolin J A and Wootters W K 1996a *Phys. Rev. Lett.* **76** 722
Bennett C H and DiVincenzo D P 2000 *Nature* **404** 247
Bennett C H, DiVincenzo D P, Smolin J A and Wootters W K 1996b *Phys. Rev.* A **54** 3824
Bennett C H and Wiesner S J 1992 *Phys. Rev. Lett.* **69** 2881
Blaauboer M and DiVincenzo D P 2005 *Phys. Rev. Lett.* **95** 160402
Blanter Y M and Büttiker M 2000 *Phys. Rep.* **336** 1
Börlin J, Belzig W and Bruder C 2002 *Phys. Rev. Lett.* **88** 197001
Boschi D, Branca S, De Martini F, Hardy L and Popescu S 1998 *Phys. Rev. Lett.* **80** 1121
Bose S and Home D 2002 *Phys. Rev. Lett.* **88** 050401
Bouchiat V, Chtchelkatchev N, Feinberg D, Lesovik G B, Martin T and Torrès J 2003 *Nanotechnology* **14** 77
Bouwmeester D, Pan J-W, Mattle K, Eibl M, Weinfurter H and Zeilinger A 1997 *Nature* **390** 575
Burkard G and Loss D 2003 *Phys. Rev. Lett.* **91** 087903
Burkard G, Loss D and DiVincenzo D P 1999 *Phys. Rev.* B **59** 2070
Burkard G, Loss D and Sukhorukov E V 2000 *Phys. Rev.* B **61** R16303 (*Preprint* cond-mat/9906071)
Büttiker M 1990 *Phys. Rev. Lett.* **65** 2901
Büttiker M 1992 *Phys. Rev.* B **46** 12485
Cerletti V, Gywat O and Loss D 2005 *Phys. Rev.* B **72** 115316
Chen Y and Webb R A 2006 *Phys. Rev. Lett.* **97** 066604
Choi B-R, Hansen A E, Kontos T, Hoffmann C, Oberholzer S, Belzig W, Schönenberger C, Akazaki T and Takayanagi H 2005 *Phys. Rev.* B **72** 024501
Choi M-S, Bruder C and Loss D 2000 *Phys. Rev.* B **62** 13569
Chtchelkatchev N M, Blatter G, Lesovik G B and Martin T 2002 *Phys. Rev.* B **66** 161320
Clauser J F and Horne M A 1974 *Phys. Rev.* D **10** 526
Costa A T and Bose S 2001 *Phys. Rev. Lett.* **87** 277901
Costa A T, Bose S and Omar Y 2006 *Phys. Rev. Lett.* **96** 230501
Devetak I, Harrow A W and Winter A 2004 *Phys. Rev. Lett.* **93** 230504
Di Lorenzo A and Nazarov Y V 2005 *Phys. Rev. Lett.* **94** 210601
DiVincenzo D P and Loss D 1999 *J. Magn. Magn. Mater.* **200** 202
Dowling M R, Doherty A C and Wiseman H M 2006 *Phys. Rev.* A **73** 052323
Dupont É and Le Hur K 2006 *Phys. Rev.* B **73** 045325
Egger R and Gogolin A 1997 *Phys. Rev. Lett.* **79** 5082
Egues J C, Burkard G and Loss D 2002 *Phys. Rev. Lett.* **89** 176401
Egues J C, Burkard G, Saraga D S, Schliemann J and Loss D 2005 *Phys. Rev.* B **72** 235326
Egues J C, Recher P, Saraga D S, Golovach V N, Burkard G, Sukhorukov E V and Loss D 2003 *Quantum Noise in Mesoscopic Physics* (*NATO Science Series* vol 97) (The Netherlands: Kluwer) pp 241–274 (*Preprint* cond-mat/0210498)
Einstein A, Podolsky B and Rosen N 1935 *Phys. Rev.* **47** 777
Ekert A K 1991 *Phys. Rev. Lett.* **67** 661
Faoro L, Taddei F and Fazio R 2004 *Phys. Rev.* B **69** 125326
Frustaglia D, Montangero S and Fazio R 2006 *Phys. Rev.* B **74** 165326
Galitski V M and Sarma S D 2004 *Phys. Rev.* B **70** 035111
Giovannetti V, Frustaglia D, Taddei F and Fazio R 2006 *Phys. Rev.* B **74** 115315
Gisin N, Ribordy G, Tittel W and Zbinden H 2002 *Rev. Mod. Phys.* **74** 145
Giuliani G F and Quinn J J 1982 *Phys. Rev.* B **26** 4421
Gunlycke D, Jefferson J H, Rejec T, Ramsak A, Pettifor D G and Briggs G A D 2006 *J. Phys.: Condens. Matter* **18** S851
Gywat O, Burkard G and Loss D 2002 *Phys. Rev.* B **65** 205329
Hanbury Brown R and Twiss R Q 1956 *Nature* **177** 27

Hanson R, Kouwenhoven L P, Petta J R, Tarucha S and Vandersypen L M K 2006 Spins in few-electron quantum dots *Rev. Mod. Phys.* submitted (*Preprint* cond-mat/0610433)
Hekking F W J, Glazman L I, Matveev K A and Shekhter R I 1993 *Phys. Rev. Lett.* **70** 4138
Henny M, Oberholzer S, Strunk C, Heinzel T, Ensslin K, Holland M and Schönenberger C 1999 *Science* **284** 296
Hohenester U 2002 *Phys. Rev.* B **66** 245323
Hong C K, Ou Z Y and Mandel L 1987 *Phys. Rev. Lett.* **59** 2044
Hu X and Das Sarma S 2004 *Phys. Rev.* B **69** 115312
Kane C, Balents L and Fisher M 1997 *Phys. Rev. Lett.* **79** 5086
Kawabata S 2001 *J. Phys. Soc. Japan* **70** 1210
Khlus V A 1987 *Zh. Eksp. Teor. Fiz.* **93** 2179
Kikkawa J M and Awschalom D D 1998 *Phys. Rev. Lett.* **80** 4313
Kikkawa J M, Smorchkova I P, Samarth N and Awschalom D D 1997 *Science* **277** 1284
Kouwenhoven L P, Schön G and Sohn L L (ed) 1997 *Mesoscopic Electron Transport* (*NATO ASI Series E* vol 345) (Dordrecht: Kluwer–Academic)
Landauer R 1989 *Physica* D **38** 226
Lesovik G, Martin T and Blatter G 2001 *Eur. Phys. J.* B **24** 287
Lesovik G B 1989 *Pis. Zh. Eksp. Teor. Fiz.* **49** 513
Lim Y L and Beige A 2005 *New J. Phys.* **7** 155
Liu R C, Odom B, Yamamoto Y and Tarucha S 1998 *Nature* **391** 263
Loss D and DiVincenzo D P 1998 *Phys. Rev.* A **57** 120
Loss D and Sukhorukov E V 2000 *Phys. Rev. Lett.* **84** 1035
Loudon R 1998 *Phys. Rev.* A **58** 4904
Mahan G D 1993 *Many Particle Physics* 2nd edn (New York: Plenum)
Maître X, Oliver W D and Yamamoto Y 2000 *Physica* E **6** 301
Martin T and Landauer R 1992 *Phys. Rev.* B **45** 1742
Mattle K, Weinfurter H, Kwiat P G and Zeilinger A 1996 *Phys. Rev. Lett.* **76** 4656
Mermin N D 1993 *Rev. Mod. Phys.* **65** 803
Oberholzer S, Bieri E, Schonenberger C, Giovannini M and Faist J 2006 *Phys. Rev. Lett.* **96** 046804
Oliver W D, Kim J, Liu R C and Yamamoto Y 1999 *Science* **284** 299
Oliver W D, Yamaguchi F and Yamamoto Y 2002 *Phys. Rev. Lett.* **88** 037901
Prada E and Sols F 2004 *Eur. Phys. J.* B **40** 379
Prada E, Taddei F and Fazio R 2005 *Phys. Rev.* B **72** 125333
Prinz G A 1998 *Science* **282** 1660
Recher P and Loss D 2002a *J. Supercond. Novel Magn.* **15** 49 (*Preprint* cond-mat/0202102)
Recher P and Loss D 2002b *Phys. Rev.* B **65** 165327
Recher P and Loss D 2003 *Phys. Rev. Lett.* **91** 267003
Recher P, Sukhorukov E V and Loss D 2001 *Phys. Rev.* B **63** 165314
Russo S, Kroug M, Klapwijk T M and Morpurgo A F 2005 *Phys. Rev. Lett.* **95** 027002
Samuelsson P, Sukhorukov E V and Büttiker M 2003 *Phys. Rev. Lett.* **91** 157002
Samuelsson P, Sukhorukov E V and Büttiker M 2004 *Phys. Rev.* B **70** 115330
San-Jose P and Prada E 2006 *Phys. Rev.* B **74** 045305
Saraga D S, Altshuler B L, Loss D. and Westervelt R M 2004 *Phys. Rev. Lett.* **92** 246803
Saraga D S, Altshuler B L, Loss D and Westervelt R M 2005 *Phys. Rev.* B **71** 045338
Saraga D S and Loss D. 2003 *Phys. Rev. Lett.* **90** 166803
Saraga D S and Loss D 2005 *Phys. Rev.* B **72** 195319
Sauret O, Feinberg D and Martin T 2004 *Phys. Rev.* B **70** 245313
Schliemann J, Cirac J I, Kus M, Lewenstein M and Loss D 2001a *Phys. Rev.* A **64** 022303
Schliemann J, Loss D and MacDonald A H 2001b *Phys. Rev.* B **63** 085311
Schrödinger E 1935 *Naturwissenschaften* **23** 807
Schulz H J 1990 *Phys. Rev. Lett.* **64** 2831
Sukhorukov E V, Burkard G and Loss D 2001 *Phys. Rev.* B **63** 125315
Taddei F, Faoro L, Prada E and Fazio R 2005 *New J. Phys.* **7** 183
Taddei F and Fazio R 2002 *Phys. Rev.* B **65** 075317
Taylor J M, Dur W, Zoller P, Yacoby A, Marcus C M and Lukin M D 2005 *Phys. Rev. Lett.* **94** 236803
Topinka M A, LeRoy B J, Shaw S E J, Heller E J, Westervelt R M, Maranowski K D and Gossard A C 2000 *Science* **289** 2323
Topinka M A, Leroy B J, Westervelt R M, Shaw S E J, Fleischmann R, Heller E J, Maranowski K D and Gossard A C 2001 *Nature* **410** 183

Torrès J and Martin T 1999 *Eur. Phys. J.* B **12** 319
Tsvelik A M 2003 *Quantum Field Theory in Condensed Matter Physics* 2nd edn (Cambridge: Cambridge University Press)
Werner R F 1989 *Phys. Rev.* A **40** 4277
Wiseman H M and Vaccaro J A 2003 *Phys. Rev. Lett.* **91** 097902
Wootters W K 1998 *Phys. Rev. Lett.* **80** 2245